

Adiabatic preparation of a cold exciton condensate

V. Shahnazaryan,^{1,2} O. Kyriienko,^{1,3,4} and I. A. Shelykh^{1,3}

¹*Science Institute, University of Iceland, Dunhagi-3, IS-107, Reykjavik, Iceland*

²*Institute of Mathematics and High Technologies,*

Russian-Armenian (Slavonic) University, Hovsep Emin 123, 0051, Yerevan, Armenia

³*Division of Physics and Applied Physics, Nanyang Technological University 637371, Singapore*

⁴*QUANTOP, Danish Quantum Optics Center, Niels Bohr Institute,*

University of Copenhagen, Blegdamsvej 17, DK-2100 Copenhagen, Denmark

(Dated: September 11, 2018)

We propose a scheme for the controllable preparation of a cold indirect exciton condensate using dipolaritonic setup with an optical pumping. Dipolaritons are bosonic quasiparticles which arise from the coupling between cavity photon (C), direct exciton (DX), and indirect exciton (IX) modes, and appear in a double quantum well embedded in a semiconductor microcavity. Controlling the detuning between modes of the system, the limiting cases of exciton-polaritons and indirect excitons can be realized. Our protocol relies on the initial preparation of an exciton polariton condensate for the far blue-detuned IX mode, with its subsequent adiabatic transformation to an indirect exciton condensate by lowering IX energy via applied electric field. The following allows for generation of a spatially localized cold exciton gas, on the contrary to currently used methods, where IX cloud appears due to diffusion of carriers from spatially separated electron- and hole-rich areas.

I. INTRODUCTION

Experimental observation of Bose-Einstein condensation (BEC)¹ in a cold atomic gas system represents a major breakthrough of contemporary condensed matter physics.^{2,3} However, while being a perfect testbed for studies of macroscopically coherent phenomena, the requirement of ultralow temperature ($< 1 \mu\text{K}$) of an atomic gas restricts its possible applications. Fortunately, this requirement can be removed in solid state setups, where condensation of excitons in semiconductor structures was theoretically predicted^{4,5} for considerably higher temperatures ($\approx 1 \text{ K}$). While unambiguous evidence of exciton condensation in a bulk and monolayer semiconductor structure is still lacking due to technological difficulties,⁶ several modifications of conventional excitonic system have shown promising results.

For instance, exciton polaritons, being a hybrid quasiparticles of coupled excitons in semiconductor quantum well and confined cavity photon,^{7,8} represent a useful setup for studies of bosonic phenomena due to large decoherence times and simplicity of experimental characterization using optical techniques. The extremely small mass of these quasiparticles allowed to rise the typical critical temperature of condensation to tens of Kelvins range,^{9–12} and in certain cases up to room temperature.^{13,14} With experimental advances the macroscopically coherent polariton gas is now routinely observed in numerous system, working both with incoherent optical^{9,10} and electrical^{15,16} pump. The unique properties of polaritons enabled observation of solitons,^{17–19} quantized vortices,^{20,21} polarization effects,^{22–25} and are considered as a platform for optical computing.^{26,27} At the same time, their short lifetime coming from cavity photon mode leakage does not allow for proper thermalization of particles, and essentially restricts the system to driven-dissipative non-equilibrium

behavior.²⁸

Another bosonic system where long-range coherence was observed is represented by spatially indirect excitons—composite electron-hole objects formed in a double quantum well.^{29–31} An intense research in this area revealed various phenomena, including ring fragmentation,^{32–34} polarization patterns and spin currents,^{35–37} electrical^{38,39} and acoustic⁴⁰ routing etc. Given the reduced spatial overlap of electron and hole wavefunctions,⁴¹ which causes long lifetime of indirect exciton ($> 100 \text{ ns}$),⁴² the efficient thermalization of particles can be achieved.³² Simultaneously, the reduced photon-exciton interaction constant complicates the optical generation and characterization of indirect exciton gas.⁴³ In particular, the common scheme for IX cloud preparation includes optical generation of holes in one quantum well and electrical injection of electron in the adjacent well.³¹ This largely impedes the spatial control of cold exciton gas, and for instance is believed to cause a fragmentation of an indirect exciton cloud.^{44,45}

Recently, the possibility to unite the subjects of exciton-polaritons and indirect excitons was attained in the system of dipolaritons.^{46,47} Being hybrid quasiparticles consisting of cavity photon (C), direct exciton (DX), and indirect exciton (IX), they share desirable properties of both polaritons and cold excitons, including enhanced interparticle interactions, enlarged lifetime, and improved optical control. The system of dipolaritons was proposed to serve as an efficient terahertz emitter,^{48–50} tunable single-photon source,⁵¹ and polarization switcher.⁵²

In this paper we propose a scheme for optical generation of a cold indirect exciton condensate using a dipolariton setup. At the first step, it requires an initial preparation of an exciton polariton condensate using the incoherent optical pump, with indirect exciton mode lying high in energy for zero applied electric field F . By lowering IX

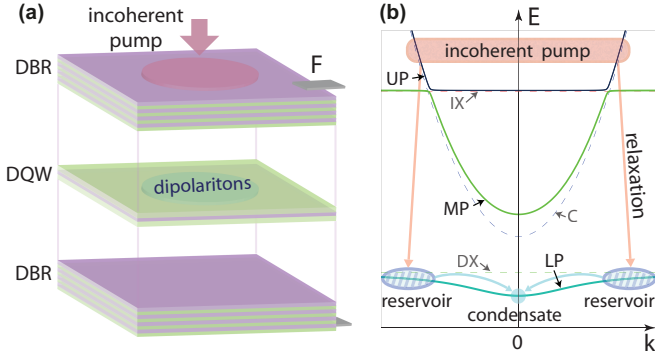


FIG. 1: (Color online) (a): Sketch of the dipolaritonic system, representing double quantum well (DQW) structure embedded in a microcavity formed by distributed Bragg reflectors (DBRs). (b): Schematic representation of dispersion of lower (LP), middle (MP), and upper (UP) dipolaritons. Incoherent optical pump creates carriers at high energy, which relax to LP reservoir, and consequently scatter to a macroscopically coherent ground state.

energy with an increase of field F , the lower dipolariton state experiences adiabatic Landau-Zener transition,^{53,54} converting to indirect excitonic state with high fidelity. The following allows for generation of a spatially localized cold exciton gas, on the contrary to currently used methods, where IX cloud appears due to diffusion of carriers from spatially separated electron- and hole-rich areas.

II. THE MODEL

The considered structure consists of two quantum wells separated by a thin barrier, allowing electron to tunnel between the wells. This double quantum well (DQW) system is placed in an optical microcavity, providing the existence of a cavity photon mode strongly coupled to a direct exciton mode, while an indirect exciton mode remains decoupled from the light mode [Fig. 1(a)]. An indirect exciton instead is coupled to direct exciton due to coherent tunnel coupling between the QWs. The bias is applied to the heterostructure in the growth direction, which allows to tune the energy of an indirect exciton and thus the tunneling efficiency.

The Hamiltonian of dipolariton system can be written in the general form $\hat{H} = \hat{H}_{\text{coh}} + \hat{H}_{\text{dec}}$, where coherent and decoherent processes are separated. The coherent part of Hamiltonian reads:

$$\begin{aligned} \hat{H}_{\text{coh}} = & \hbar\omega_C \hat{a}^\dagger \hat{a} + \hbar\omega_{DX} \hat{b}^\dagger \hat{b} + \hbar\omega_{IX}(t) \hat{c}^\dagger \hat{c} \\ & + \frac{\hbar\Omega}{2} (\hat{a}^\dagger \hat{b} + \hat{b}^\dagger \hat{a}) - \frac{\hbar J}{2} (\hat{b}^\dagger \hat{c} + \hat{c}^\dagger \hat{b}), \end{aligned} \quad (1)$$

where \hat{a}^\dagger , \hat{b}^\dagger and \hat{c}^\dagger are creation operators of cavity photons, direct excitons, and indirect excitons, respectively. First three terms in Eq. (1) correspond to energies of photon ($\hbar\omega_C$), direct exciton ($\hbar\omega_{DX}$) and indirect exciton ($\hbar\omega_{IX}$) modes. The next two terms describe the

direct exciton-cavity photon Rabi splitting $\hbar\Omega$ and the direct-indirect exciton tunneling splitting $\hbar J$. Here, we emphasize that an indirect exciton energy is time dependent, and depends linearly on the time-varied applied electric field $F(t)$, $\hbar\omega_{IX}(t) = \hbar\omega_{IX}^{(0)} - eLF(t)$. This expression hold for narrow QW heterostructure; $\hbar\omega_{IX}^{(0)}$ is an energy of indirect exciton at zero bias; L is a distance between centers of QWs; e denotes electron charge.

For the strong coupling case where intermode couplings Ω and J overcome decay (or broadening) of the modes, the eigenstates of Hamiltonian (1) correspond to lower (LP), middle (MP), and upper (UP) dipolariton states, being coherent superpositions of original C, DX, and IX states. The sketch of dipolariton dispersions is shown in Fig. 1(b) for largely blue-detuned indirect exciton mode, and positive detuning of cavity photon with respect to direct exciton, $\omega_C - \omega_{DX} > 0$.

The initial feeding source of the dipolariton system is represented by laser tuned to high energies [Fig. 1(b)]. It excites free electrons and holes, which relax to low energies, forming excitons with large wave vectors, commonly referred as reservoir states.⁵⁵ During this fast relaxation process the initial phase of the laser is fully lost, and incoherent reservoir of the direct excitons is created. Next, the excitons from reservoir can scatter due to exciton-phonon interactions towards ground state at zero wave vector of lower dipolariton mode, where they form a macroscopically occupied coherent state. The following excitation scheme is commonly used in conventional polaritonic setups,⁹ where nonequilibrium condensation of polaritons under incoherent pumping conditions was observed.

To describe incoherent processes related to phonon-assisted scattering of particles from reservoir to the ground state, we introduce the exciton-phonon interaction Hamiltonian $\hat{H}_{\text{dec}} = \hat{H}^+ + \hat{H}^-$, where

$$\hat{H}^+ = D_{ph} \sum_k \hat{b}^\dagger \hat{r}_k \hat{d}_k^\dagger; \quad \hat{H}^- = D_{ph} \sum_k \hat{b} \hat{r}_k^\dagger \hat{d}_k, \quad (2)$$

correspond to processes with emission (\hat{d}_k^\dagger) and absorption (\hat{d}_k) of phonons with wave vector k . \hat{r}_k^\dagger and \hat{r}_k are creation and annihilation operators for reservoir states. D_{ph} denotes exciton-phonon interaction constant.

In order to take into account the decoherence caused by a finite lifetime of the modes and interaction with reservoir, one can use the Lindblad master equation for the density matrix ρ ,

$$\frac{\partial \rho}{\partial t} = \frac{i}{\hbar} [\rho, \hat{H}] + \hat{\mathcal{L}}^{(\text{dis})} \rho + \hat{\mathcal{L}}^{(\text{th})} \rho, \quad (3)$$

where $\hat{\mathcal{L}}^{(\text{dis})}$ is Lindblad superoperator having the form $\hat{\mathcal{L}}^{(\text{dis})} \rho = \sum_i \gamma_i (\hat{a}_i \rho \hat{a}_i^\dagger - \{\hat{a}_i^\dagger \hat{a}_i, \rho\}/2)$ with $\hat{a}_i = \hat{a}, \hat{b}, \hat{c}$ and $\gamma_j = 1/\tau_j$ ($j = C, DX, IX$) being damping rates of the modes.⁴⁸ The term $\hat{\mathcal{L}}^{(\text{th})} \rho$ corresponds to phonon-assisted processes accounted using Born-Markov approximation.⁵⁶

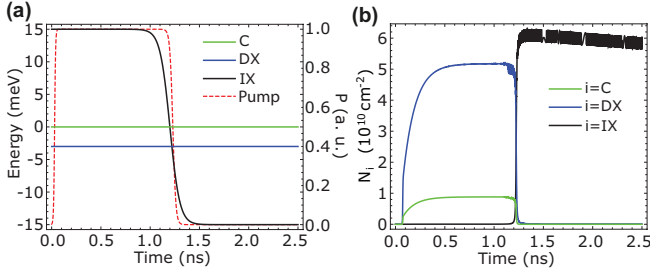


FIG. 2: (Color online) (a): Time dependence of energies of the modes. The bias applied to the system causes linear decrease of IX energy in $t = 1$ ns to $t = 1.5$ ns window, up to far red-detuned value. The dashed red line corresponds to time dependence of the pump intensity (in arbitrary units). (b): The evolution of occupations of the modes, being $N_C = |\langle \hat{a} \rangle|^2$, $N_{DX} = |\langle \hat{b} \rangle|^2$, and $N_{IX} = |\langle \hat{c} \rangle|^2$. At the first stage ($t < 1$ ns) the formation of polariton condensate takes place. Next, continuous change of an applied bias drives the system through an avoided crossing, leading to the transfer of polariton occupation to an indirect exciton mode.

Since we are interested in a large number of particles, we can apply the mean field approximation when time dynamics of the system can be defined by equations for mean fields given by $\partial \langle \hat{a}_i \rangle / \partial t = \text{Tr}(\hat{a}_i \partial \rho / \partial t)$, where $\hat{a}_i = \hat{a}, \hat{b}, \hat{c}$.

Using the straightforward algebra we get equations of motions for the cavity photon, direct exciton, and indirect fields coupled to reservoir:⁵⁶

$$\frac{\partial \langle \hat{a} \rangle}{\partial t} = -i\omega_C \langle \hat{a} \rangle - i\frac{\Omega}{2} \langle \hat{b} \rangle - \frac{\gamma_C}{2} \langle \hat{a} \rangle, \quad (4)$$

$$\begin{aligned} \frac{\partial \langle \hat{b} \rangle}{\partial t} &= -i\omega_{DX} \langle \hat{b} \rangle - \frac{\Omega}{2} \langle \hat{a} \rangle + i\frac{J}{2} \langle \hat{c} \rangle - \frac{\gamma_{DX}}{2} \langle \hat{b} \rangle \\ &+ \frac{W}{2} \langle \hat{b} \rangle (N_R - N_{ph}), \end{aligned} \quad (5)$$

$$\frac{\partial \langle \hat{c} \rangle}{\partial t} = -i\omega_{IX}(t) \langle \hat{c} \rangle + i\frac{J}{2} \langle \hat{b} \rangle - \frac{\gamma_{IX}}{2} \langle \hat{c} \rangle, \quad (6)$$

$$\frac{\partial N_R}{\partial t} = P(t) - \gamma_R N_R - W |\langle \hat{b} \rangle|^2 (N_R - N_{ph}), \quad (7)$$

where $N_R = \sum_k n_k^R \equiv \sum_k \langle \hat{r}_k^\dagger \hat{r}_k \rangle$ denotes the full occupancy of the reservoir and $N_{ph} = \sum_k n_k^{ph}$ corresponds to the total number of the phonons defined by the temperature of the sample. $W = 2\delta_R D_{ph}^2$ corresponds to the scattering rate of reservoir particles to macroscopically coherent state, where δ_R is the inverse broadening of exciton states divided by \hbar^2 . The term $P(t)$ in Eq. (7) corresponds to the incoherent pump of reservoir states, which is typically given by the Lindblad type operator written in the form:

$$\hat{\mathcal{L}}^{(\text{pump})} \rho = \sum_k P_k(t) \left(\hat{r}_k \rho \hat{r}_k^\dagger + \hat{r}_k^\dagger \rho \hat{r}_k - \hat{r}_k^\dagger \hat{r}_k \rho - \rho \hat{r}_k^\dagger \hat{r}_k \right), \quad (8)$$

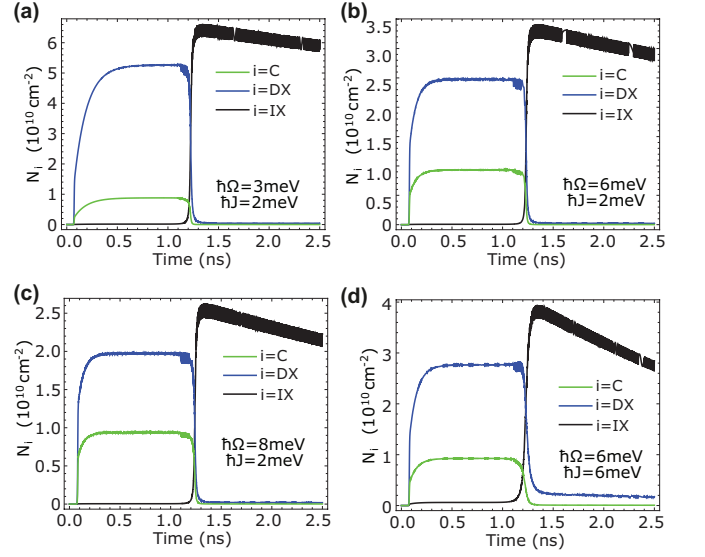


FIG. 3: (Color online) Transition dynamics shown for different coupling parameters Ω and J . (a, b, c): Tunneling coupling is fixed to $\hbar J = 2$ meV ($L_b = 8$ nm), while Rabi splitting is equal to $\hbar\Omega = 3$ meV (a), $\hbar\Omega = 6$ meV (b), and $\hbar\Omega = 8$ meV (c). (d): Occupation transfer in the system with equal couplings, $\hbar J = \hbar\Omega = 6$ meV.

where $|P_k(t)|^2$ denotes the intensity of incoherent pump of single reservoir state with in-plane wave vector k , and total pump is defined as $P(t) = \sum_k P_k(t)$. Writing the system of the kinetic equations we assumed large occupancy of the condensate state thus neglecting terms corresponding to spontaneous scattering. We checked numerically that these terms do not affect the obtained results.

III. RESULTS AND DISCUSSION

We simulate the dipolariton system based on $\text{In}_{0.1}\text{Ga}_{0.9}\text{As}/\text{GaAs}/\text{In}_{0.08}\text{Ga}_{0.92}\text{As}$ heterostructure.⁴⁶ The coupling parameters are chosen as $\hbar\Omega = 3$ meV and $\hbar J = 1$ meV. The latter corresponds to DQW with barrier width of $L_b = 10$ nm. Lifetimes of the modes are chosen as $\tau_C = 20$ ps, $\tau_{DX} = 1$ ns, $\tau_{IX} = 100$ ns. The damping rate of reservoir states $\gamma_R = 1/\tau_R$ is defined by lifetime $\tau_R = 0.1$ ns. Initially, at zero applied field energies of the modes system are tuned to $\hbar\omega_{DX} - \hbar\omega_C = -3$ meV, $\hbar\omega_{IX}^{(0)} - \hbar\omega_C = 15$ meV, and we set the reference point $\hbar\omega_C = 0$ without loss of generality [see Fig. 2(a) for $t \rightarrow 0$]. The reservoir scattering rate $W = 1/\tau_{sc}$ is defined by characteristic exciton-phonon scattering time τ_{sc} , and chosen as 200 ps.^{57,58} The temperature of the sample was assumed to be $T = 0.7$ K, being typical for experiments with cold indirect excitons.³⁰

We start switching on incoherent pump $P(t)$ gradually [Fig. 2(a)], populating reservoir exciton states. Due to

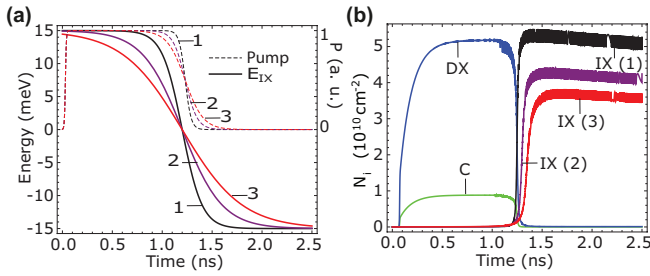


FIG. 4: (Color online) IX mode dynamics for different adiabaticity parameters. (a): Time dependence of IX mode energy (solid curves, left scale) and pump intensity (dashed curves, right scale). Three different regimes correspond to switching times $\Delta\tau_{1,2,3} = 100, 200, 300$ ps. (b): Occupation number dynamics of the modes shown for different switching regimes. The dynamics of C and DX modes remains unchanged, while the final occupation of IX mode strongly depends on switching parameters.

phonon-exciton interaction particles from reservoir thermalize and scatter to lowest energy state of lower dipolariton branch during several hundreds of picoseconds, where the steady-state is achieved approximately at 0.5 ns [Fig. 2(b)]. By this moment the DX mode is highly populated, while IX mode remains empty due to large separation in energy and smallness of interaction with reservoir. The crucial idea now is to change the bias applied to the system. The IX mode energy then varies linearly up to large red-detuned value [$\hbar\omega_{IX}^{(\infty)} = -15$ meV], while direct exciton and cavity photon modes energies remain unchanged. The exact shape of IX energy dependence is plotted in Fig. 2(a), and is described by formula $\hbar\omega_{IX}(t) = \left(\hbar\omega_{IX}^{(0)} - \hbar\omega_{IX}^{(\infty)} \right) / \left(1 + \exp^{[t-\tau]/\Delta\tau} \right) + \hbar\omega_{IX}^{(\infty)}$, where parameters are $\tau = 1200$ ps and $\Delta\tau = 50$ ps.

If one changes the bias slowly, the Landau-Zener type transition between bosonic modes takes place. Namely, the system adiabatically follows the lower dipolariton branch, and at the final stage of complete swap gains 99.9% indirect exciton fraction. Alias, in the basis of bare modes the IX population largely increases due to transfer from cavity photon and direct exciton (polariton) modes, where their occupations drop to zero [Fig. 2(b), after 1.3 ns]. This corresponds to conversion of macroscopically coherent polariton population to a gas of cold indirect excitons, which inherit coherence properties and demonstrate long lifetime (characteristic decay time > 10 ns for chosen parameters).

We note that successive preparation of cold exciton BEC requires simultaneous switching off the pump $P(t)$, leading to the rapid devastation of the reservoir mode. The following allows to keep high transfer fidelity, where overall particle occupation remains large during the transfer event, but prevents refilling of polaritonic states.

To characterize the system and find optimal parameters for cold exciton condensate preparation, we proceed

considering different coupling parameters of dipolariton setup. In Fig. 3 the transition process is demonstrated for several values of Rabi frequency Ω and tunneling splitting J . First, we fix tunneling constant to $\hbar J = 2$ meV (as in Fig. 2) and vary the strength of light-matter interaction. We find that increase of Rabi frequency Ω causes the reduction of transition efficiency, which can be clearly observed in Figs. 3(a), (b), and (c). First, this can be linked to increase of cavity photon admixture in the lower dipolariton mode, and consequent enlargement of decay. Second, the change of coupling Ω in general strongly influences Landau-Zener transition in three-mode system.

In Fig. 3(d) we show the population transfer for the case of equal couplings $\hbar J = \hbar\Omega = 6$ meV, corresponding to the sample discussed in the Ref. [46]. We observe that population transfer for these parameters is not perfect, and thus conclude that $J < \Omega$ condition shall be followed. Furthermore, we note that large values of tunneling constant J lead to stronger mixing of IX and DX modes, with consequent decrease of the lower dipolariton lifetime after switching.

Next, we study the influence of electric field switching process on the performance of population transfer. The main parameter here is a switching time τ , which also determines the switching rate $c = \Delta\tau^{-1}/4$ at which energy linearly decreases as $\sim -ct$ around transition point τ . It defines the adiabaticity of transition, and is of high importance for successive Landau-Zener transition. In particular, the optimal transfer requires slow variation of detuning, as compared to the energy distance between modes in the anticrossing point of dressed modes.

In Fig. 4 the time dynamics of the system is presented for different switching rates. We considered three regimes, altering both the rate of detuning switching and the front of pump switching, in order to keep density of the particles at the same level [Fig. 4(a)]. We find that the voltage switching rate almost does not affect on the polariton population at steady-state condition, but strongly influences the efficiency of the transition, defining the IX mode occupation [Fig. 4(b)]. For the switching time $\Delta\tau_1 = 100$ ps nearly perfect transfer was achieved. This confirms that the characteristic time corresponding to anticrossing energy distance is ~ 1 ps, and transition is adiabatic. However, decreasing the switching rate to $\Delta\tau_2 = 200$ ps and $\Delta\tau_3 = 300$ ps we revealed the reduction of transfer efficiency, signifying of an existence of an optimal rate $\Delta\tau$. The process of spoiling of transition is related to open-dissipative nature of the system under the study.

Finally, we acknowledge the presence of another bound which puts limitation on detuning switching rate. It comes from the experimental limitation of DC voltage sweep rate, which typically cannot outperform gigahertz repetition rates. While state-of-the-art devices with fast switching are currently engineered,⁵⁹ we probe the possibility to decrease the sweep rate up to 100 MHz range. In Fig. 5 we show that the transition can take place for switching time being in the tens of nanoseconds range

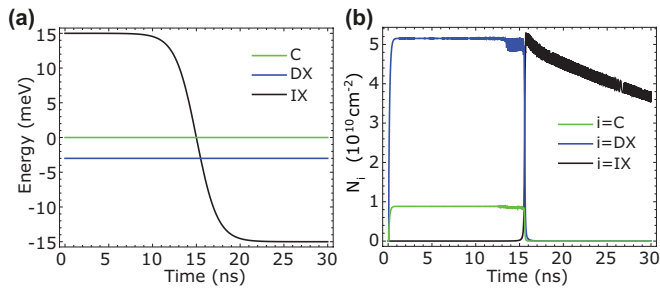


FIG. 5: (Color online) (a): Time dependence of energy of the modes for modified dipolariton system, where ultra-slow change of detuning is implemented. (b): Population transfer in dipolariton system for ultra-slow detuning change. Parameters of the calculation are: $\tau = 15$ ns, $\Delta\tau = 1.2$ ns.

[Fig. 5(a)], easily achievable with current technologies. The transition efficiency in this case drops as opposed to less-than-nanosecond switching time. At the same time, a decent population of indirect exciton gas can be achieved for certain pumping conditions, which persists for tens of nanoseconds. The parameters of the system for this calculation were modified to $\hbar J = 0.6$ meV and $\hbar\Omega = 3$ meV.

Finally, let us discuss the immediate consequences of proposed scheme for cold exciton gas preparation. Being based on conversion of optically created polaritons to an indirect exciton gas, it ensures the preservation of the spatial shape of initial cloud, and does not involve separate injection of electron and hole carriers. This is in contrast to typical excitation scheme in the indirect exciton experiments, where optical generation of holes and electrical injection of electrons is used.^{30,31} The following allows to test the possible explanation of IX ring appearance based on the electrostatic reasoning.^{44,45}

Moreover, we note that our proposal can be tested in first approximation even without the presence of an optical microresonator. In this case only coupled DX and

IX modes are considered, and conversion of optically active direct excitons to a cloud of indirect excitons can be realized. However, on the contrary to the full dipolaritonic setup, no condensation effects for direct excitons are expected which can limit the efficiency of the proposed protocol.

IV. CONCLUSIONS

In conclusion, we proposed the way for an on-demand optical preparation of a cold exciton condensate based on Landau-Zener bosonic transfer in a dipolariton system. The protocol is based on several steps. First stage corresponds to initial preparation of polariton condensate with high cavity photon and direct exciton fractions, while indirect exciton mode is located high in energy at zero external voltage. Next, applying electric field the IX energy is lowered to far red-detuned value, where adiabatic following of the lower dipolariton mode converts particles to indirect excitons with inherited coherence properties. Finally, to reduce residual effects of cavity an optical incoherent pump of polaritonic reservoir states shall be switched off during the transfer event. We analyzed the population transfer for various sets of parameters and switching conditions, and demonstrated that adiabatic cold exciton preparation is experimentally feasible in currently existing setups.

Acknowledgements

We thank S. A. Tarasenko, S. Morina, and H. Sigurdson for the useful discussions. The work was supported by the Tier 1 project Polaritons for novel device applications, FP7 IRSES projects POLAPHEN, POLATER and QOCaN, and FP7 ITN NOTEDEV network.

¹ L. Pitaevskii and S. Stringari, *Bose-Einstein Condensation* (Oxford University Press, Oxford, 2003).

² M. H. Anderson, J. R. Ensher, M. R. Matthews, C. E. Wieman, and E. A. Cornell, *Science* **269**, 198 (1995).

³ K. B. Davis, M.-O. Mewes, M. R. Andrews, N. J. van Druten, D. S. Durfee, D. M. Kurn, and W. Ketterle, *Phys. Rev. Lett.* **75**, 3969 (1995).

⁴ L. V. Keldysh and Yu. V. Kopayev, *Sov. Phys. Solid State* **6**, 2219 (1965); L. V. Keldysh and A. N. Kozlov, *Sov. Phys. JETP* **27**, 521 (1968).

⁵ J. M. Blatt, K. W. Böer, and W. Brandt, *Phys. Rev.* **126**, 1691 (1962).

⁶ S. A. Moskalenko and D. W. Snoke, *Bose-Einstein Condensation of Excitons and Biexcitons* (Cambridge University Press, Cambridge, U.K., 2000).

⁷ A. V. Kavokin, J. J. Baumberg, G. Malpuech, and F. P. Laussy, *Microcavities* (Oxford University Press, New York,

2007).

⁸ H. Deng, H. Haug, and Y. Yamamoto, *Rev. Mod. Phys.* **82**, 1489 (2010).

⁹ J. Kasprzak, M. Richard, S. Kundermann, A. Baas, P. Jeambrun, J. M. J. Keeling, F. M. Marchetti, M. H. Szymanska, R. Andre, J. L. Staehli, V. Savona, P. B. Littlewood, B. Deveaud, and Le Si Dang, *Nature (London)* **443**, 409 (2006).

¹⁰ R. Balili, V. Hartwell, D. Snoke, L. Pfeiffer, and K. West, *Science* **316**, 1007 (2007).

¹¹ E. Wertz, L. Ferrier, D. D. Solnyshkov, R. Johne, D. Sanvitto, A. Lemaître, I. Sagnes, R. Grousson, A. V. Kavokin, P. Senellart, G. Malpuech, and J. Bloch, *Nature Phys.* **6**, 860 (2010).

¹² J. Fischer, S. Brodbeck, A.V. Chernenko, I. Lederer, A. Rahimi-Iman, M. Amthor, V.D. Kulakovskii, L. Worschech, M. Kamp, M. Durnev, C. Schneider, A. V.

- Kavokin, and S. Höfling, *Phys. Rev. Lett.* **112**, 093902 (2014).
- ¹³ J. J. Baumberg, A. V. Kavokin, S. Christopoulos, A. J. D. Grundy, R. Butté, G. Christmann, D. D. Solnyshkov, G. Malpuech, G. Baldassarri Höger von Hogersthal, E. Feltin, J.-F. Carlin, and N. Grandjean, *Phys. Rev. Lett.* **101**, 136409 (2008).
- ¹⁴ J. D. Plumhof, T. Stöferle, L. Mai, U. Scherf, and R. F. Mahrt, *Nature Mater.* **13**, 247 (2014).
- ¹⁵ C. Schneider, A. Rahimi-Iman, Na Young Kim, J. Fischer, I. G. Savenko, M. Amthor, M. Lerner, A. Wolf, L. Worschech, V. D. Kulakovskii, I. A. Shelykh, M. Kamp, S. Reitzenstein, A. Forchel, Y. Yamamoto, and S. Höfling, *Nature (London)* **497**, 348 (2013).
- ¹⁶ P. Bhattacharya, B. Xiao, A. Das, S. Bhowmick, and J. Heo, *Phys. Rev. Lett.* **110**, 206403 (2013).
- ¹⁷ M. Sich, D. N. Krizhanovskii, M. S. Skolnick, A. V. Gorbach, R. Hartley, D. V. Skryabin, E. A. Cerda-Méndez, K. Biermann, R. Hey, and P. V. Santos, *Nature Photon.* **6**, 50 (2012).
- ¹⁸ M. Sich, F. Frasc, J. K. Chana, M. S. Skolnick, D. N. Krizhanovskii, A. V. Gorbach, R. Hartley, D. V. Skryabin, S. S. Gavrilov, E. A. Cerda-Méndez, K. Biermann, R. Hey, and P. V. Santos, *Phys. Rev. Lett.* **112**, 046403 (2014).
- ¹⁹ A. Amo, S. Pigeon, D. Sanvitto, V. G. Sala, R. Hivet, I. Carusotto, F. Pisanello, G. Leménager, R. Houdré, E. Giacobino, C. Ciuti, and A. Bramati, *Science* **332**, 1167 (2011).
- ²⁰ K. G. Lagoudakis, M. Wouters, M. Richard, A. Baas, I. Carusotto, R. André, Le Si Dang, and B. Deveaud-Plédran, *Nature Phys.* **4**, 706 (2008).
- ²¹ F. Manni, K. G. Lagoudakis, T. C. H. Liew, R. André, V. Savona, and B. Deveaud, *Nature Commun.* **3**, 1309 (2012); doi:10.1038/ncomms2310.
- ²² C. Leyder, M. Romanelli, J. Ph. Karr, E. Giacobino, T. C. H. Liew, M. M. Glazov, A. V. Kavokin, G. Malpuech, and A. Bramati, *Nature Phys.* **3**, 628 (2007).
- ²³ G. Tosi, F. M. Marchetti, D. Sanvitto, C. Antón, M. H. Szymańska, A. Berceanu, C. Tejedor, L. Marrucci, A. Lemaître, J. Bloch, and L. Vina, *Phys. Rev. Lett.* **107**, 036401 (2011).
- ²⁴ C. Adrados, A. Amo, T. C. H. Liew, R. Hivet, R. Houdré, E. Giacobino, A. V. Kavokin, and A. Bramati, *Phys. Rev. Lett.* **105**, 216403 (2010).
- ²⁵ I. A. Shelykh, A. V. Kavokin, Y. G. Rubo, T. C. H. Liew, and G. Malpuech, *Semicond. Sci. Technol.* **25**, 013001 (2010).
- ²⁶ T. Espinosa-Ortega and T. C. H. Liew, *Phys. Rev. B* **87**, 195305 (2013).
- ²⁷ T. C. H. Liew, A. V. Kavokin, T. Ostatnický, M. Kalitchevski, I. A. Shelykh, and R. A. Abram, *Phys. Rev. B* **82**, 033302 (2010).
- ²⁸ I. Carusotto and C. Ciuti, *Rev. Mod. Phys.* **85**, 299 (2013).
- ²⁹ A. A. High, J. R. Leonard, A. T. Hammack, M. M. Fogler, L. V. Butov, A. V. Kavokin, K. L. Campman, and A. C. Gossard, *Nature (London)* **483**, 584 (2012).
- ³⁰ L. V. Butov, *J. Phys.: Condens. Matter* **16**, R1577 (2004).
- ³¹ L. V. Butov, *J. Phys. Condens. Matter* **19**, 295202 (2007).
- ³² L. V. Butov, A. C. Gossard, and D. S. Chemla, *Nature* **418**, 751 (2002).
- ³³ D. Snoke, S. Denev, Y. Liu, L. Pfeiffer, and K. West, *Nature* **418**, 754 (2002).
- ³⁴ M. Alloing, D. Fuster, Y. González, L. González, and F. Dubin, arXiv:1210.3176 (2012).
- ³⁵ A. A. High, A. T. Hammack, J. R. Leonard, Sen Yang, L. V. Butov, T. Ostatnický, M. Vladimirova, A. V. Kavokin, T. C. H. Liew, K. L. Campman, and A. C. Gossard, *Phys. Rev. Lett.* **110**, 246403 (2013).
- ³⁶ J. R. Leonard, Y. Y. Kuznetsova, Sen Yang, L. V. Butov, T. Ostatnický, A. Kavokin, and A. C. Gossard, *Nano Lett.* **9**, 4204 (2009).
- ³⁷ A. Violante, R. Hey, and P. V. Santos, arXiv:1408.4547 (2014).
- ³⁸ A. G. Winbow, J. R. Leonard, M. Remeika, Y. Y. Kuznetsova, A. A. High, A. T. Hammack, L. V. Butov, J. Wilkes, A. A. Guenther, A. L. Ivanov, M. Hanson, and A. C. Gossard, *Phys. Rev. Lett.* **106**, 196806 (2011).
- ³⁹ P. Andreakou, S. V. Poltavtsev, J. R. Leonard, E. V. Calman, M. Remeika, Y. Y. Kuznetsova, L. V. Butov, J. Wilkes, M. Hanson, and A. C. Gossard, *Appl. Phys. Lett.* **104**, 091101 (2014).
- ⁴⁰ S. Lazić, A. Violante, K. Cohen, R. Hey, R. Rapaport, and P. V. Santos, *Phys. Rev. B* **89**, 085313 (2014).
- ⁴¹ K. Sivalertporn, L. Mouchliadis, A. L. Ivanov, R. Philp, and E. A. Muljarov, *Phys. Rev. B* **85**, 045207 (2012).
- ⁴² L. V. Butov, A. L. Ivanov, A. Imamoglu, P. B. Littlewood, A. A. Shashkin, V. T. Dolgoplov, K. L. Campman, and A. C. Gossard, *Phys. Rev. Lett.* **86**, 5608 (2001).
- ⁴³ A. V. Nalitov, M. Vladimirova, A. V. Kavokin, L. V. Butov, and N. A. Gippius, *Phys. Rev. B* **89**, 155309 (2014).
- ⁴⁴ L. V. Butov, L. S. Levitov, A. V. Mintsev, B. D. Simons, A. C. Gossard, and D. S. Chemla, *Phys. Rev. Lett.* **92**, 117404 (2004).
- ⁴⁵ R. Rapaport, Gang Chen, D. Snoke, Steven H. Simon, Loren Pfeiffer, Ken West, Y. Liu, and S. Denev, *Phys. Rev. Lett.* **92**, 117405 (2004).
- ⁴⁶ P. Cristofolini, G. Christmann, S. I. Tsintzos, G. Deligeorgis, G. Konstantinidis, Z. Hatzopoulos, P. G. Savvidis, and J. J. Baumberg, *Science* **336**, 704 (2012).
- ⁴⁷ G. Christmann, A. Askitopoulos, G. Deligeorgis, Z. Hatzopoulos, S. I. Tsintzos, P. G. Savvidis, and J. J. Baumberg, *Appl. Phys. Lett.* **98**, 081111 (2011).
- ⁴⁸ O. Kyriienko, A. V. Kavokin, and I. A. Shelykh, *Phys. Rev. Lett.* **111**, 176401 (2013).
- ⁴⁹ K. Kristinsson, O. Kyriienko, T. C. H. Liew, and I. A. Shelykh, *Phys. Rev. B* **88**, 245303 (2013).
- ⁵⁰ K. Kristinsson, O. Kyriienko, and I. A. Shelykh, *Phys. Rev. A* **89**, 023836 (2014).
- ⁵¹ O. Kyriienko, I. A. Shelykh, and T. C. H. Liew, *Phys. Rev. A* **90**, 033807 (2014).
- ⁵² A. Nalitov, D. Solnyshkov, N. Gippius, and G. Malpuech, *Proceeding of PLMCN2014*, Montpellier, France.
- ⁵³ N. A. Sinitsyn, *Phys. Rev. A* **87**, 032701 (2013).
- ⁵⁴ T. C. H. Liew and I. A. Shelykh, *J. Phys. B: At. Mol. Opt. Phys.* **45**, 245003 (2012).
- ⁵⁵ M. Wouters and I. Carusotto, *Phys. Rev. Lett.* **99**, 140402 (2007).
- ⁵⁶ See Supplemental Material [online] for the details of derivation.
- ⁵⁷ S. Huppert, O. Lafont, E. Baudin, J. Tignon and R. Ferreira, arXiv:1409.2780v1.
- ⁵⁸ F. Tassone, C. Piermarocchi, V. Savona, A. Quattropani, and P. Schwendimann, *Phys. Rev. B* **53**, R7642 (1996).
- ⁵⁹ M. Tonouchi, *Nature Photonics* **1**, 97 (2007).

Supplemental Material: Adiabatic preparation of a cold exciton condensate

V. Shahnazaryan,¹ O. Kyriienko,^{1,2,3} and I. A. Shelykh^{1,2}

¹Science Institute, University of Iceland, Dunhagi-3, IS-107, Reykjavik, Iceland

²Division of Physics and Applied Physics, Nanyang Technological University 637371, Singapore

³QUANTOP, Danish Quantum Optics Center, Niels Bohr Institute, University of Copenhagen, Blegdamsvej 17, DK-2100 Copenhagen, Denmark

(Dated: September 11, 2018)

Appendix A: Equations of motion in first order mean field theory

Here we present the derivation of equations for time dynamics of the system [Eqs. (4)-(7) in the main text].

Coherent part. The coherent part of dynamics for cavity photon occupation number $\langle \hat{a} \rangle$ can be found as

$$\begin{aligned} \left. \frac{\partial \langle \hat{a} \rangle}{\partial t} \right|_{coh} &= \frac{i}{\hbar} \text{Tr} \{ \hat{a} [\rho, \hat{H}_{coh}] \} = \frac{i}{\hbar} \text{Tr} \{ \rho [\hat{H}_{coh}, \hat{a}] \} \quad (\text{A1}) \\ &= \frac{i}{\hbar} \text{Tr} \{ \rho (-\hbar \omega_C \hat{a} - \frac{\hbar \Omega}{2} \hat{b}) \} = -i \omega_C \langle \hat{a} \rangle - i \frac{\Omega}{2} \langle \hat{b} \rangle. \end{aligned}$$

In the same fashion for expectation values of operators \hat{b} , \hat{c} we have

$$\left. \frac{\partial \langle \hat{b} \rangle}{\partial t} \right|_{coh} = -i \omega_{DX} \langle \hat{b} \rangle - i \frac{\Omega}{2} \langle \hat{a} \rangle + i \frac{J}{2} \langle \hat{c} \rangle, \quad (\text{A2})$$

$$\left. \frac{\partial \langle \hat{c} \rangle}{\partial t} \right|_{coh} = -i \omega_{IX} \langle \hat{c} \rangle + i \frac{J}{2} \langle \hat{b} \rangle. \quad (\text{A3})$$

Dissipation. To describe the incoherent processes the master equation approach with dissipators written in Lindblad form can be used.¹ Particularly, the decay of cavity mod can be treated as

$$\begin{aligned} \left. \frac{\partial \langle \hat{a} \rangle}{\partial t} \right|_{dis} &= \text{Tr} \{ \hat{a} \hat{\mathcal{L}}_a^{(dis)} \rho \} = \text{Tr} \{ \hat{a} \frac{\gamma_C}{2} (2 \hat{a} \rho \hat{a}^\dagger - \hat{a}^\dagger \hat{a} \rho - \rho \hat{a}^\dagger \hat{a}) \} \\ &= \frac{\gamma_C}{2} \text{Tr} \{ 2 \rho \hat{a}^\dagger \hat{a} \hat{a} - \rho \hat{a} \hat{a}^\dagger \hat{a} - \rho \hat{a}^\dagger \hat{a} \hat{a} \} = -\frac{\gamma_C}{2} \langle \hat{a} \rangle. \end{aligned} \quad (\text{A4})$$

Similarly,

$$\begin{aligned} \left. \frac{\partial \langle \hat{b} \rangle}{\partial t} \right|_{dis} &= -\frac{\gamma_{DX}}{2} \langle \hat{b} \rangle, \\ \left. \frac{\partial \langle \hat{c} \rangle}{\partial t} \right|_{dis} &= -\frac{\gamma_{IX}}{2} \langle \hat{c} \rangle, \\ \left. \frac{\partial n_R}{\partial t} \right|_{dis} &= -\gamma_R n_R. \end{aligned} \quad (\text{A5})$$

Interaction with reservoir. The dynamics of the system caused by interaction with exciton reservoir can be calculated in Born-Markov approximation as

$$\left. \frac{\partial \langle \hat{b} \rangle}{\partial t} \right|_{int} = \delta_{\Delta E} \left\{ \left\langle \left[\hat{H}^-, [\hat{b}, \hat{H}^+] \right] \right\rangle + \left\langle \left[\hat{H}^+, [\hat{b}, \hat{H}^-] \right] \right\rangle \right\}, \quad (\text{A6})$$

where δ_R is inverse broadening of exciton states divided by \hbar^2 . Calculation of commutators one by one gives $[\hat{b}, \hat{H}^-] = 0$, $[\hat{b}, \hat{H}^+] = R_{ph} \sum_k \hat{r}_k \hat{d}_k^\dagger$, $[\hat{H}^+, [\hat{b}, \hat{H}^-]] = R_{ph}^2 \sum_k (\hat{r}_k^\dagger \hat{r}_k - \hat{d}_k^\dagger \hat{d}_k) \hat{b}$. Finally,

$$\begin{aligned} \left. \frac{\partial \langle \hat{b} \rangle}{\partial t} \right|_{int} &= \delta_{\Delta E} R_{ph}^2 \sum_k (n_k^R - n_k^{ph}) \langle \hat{b} \rangle \quad (\text{A7}) \\ &= \delta_{\Delta E} R_{ph}^2 \left(N_R - \sum_k n_k^{ph} \right) \langle \hat{b} \rangle. \end{aligned}$$

In the same way for reservoir states we get

$$\begin{aligned} \left. \frac{\partial N_R}{\partial t} \right|_{int} &= \sum_k \left. \frac{\partial n_k^R}{\partial t} \right|_{int} \quad (\text{A8}) \\ &= \sum_k \left\{ \left\langle \left[\hat{H}^-, [\hat{r}_k^\dagger \hat{r}_k, \hat{H}^+] \right] \right\rangle + \left\langle \left[\hat{H}^+, [\hat{r}_k^\dagger \hat{r}_k, \hat{H}^-] \right] \right\rangle \right\} \end{aligned}$$

$$= -2 \delta_{\Delta E} R_{ph}^2 \left(|\langle \hat{b} \rangle|^2 N_R + \sum_k [(n_k^{ph} + 1) n_k^R - |\langle \hat{b} \rangle|^2 n_k^{ph}] \right).$$

Here the relevant term corresponds to the stimulated scattering between reservoir and coherent mode, while spontaneous scattering can be usually neglected.

Incoherent pump. The pump of reservoir can be introduced using the Lindblad superoperator for incoherent pumping of each reservoir state with momentum q , and is given by:²

$$\left. \frac{\partial n_q^R}{\partial t} \right|_{pump} = \text{Tr} \left\{ \hat{r}_q^\dagger \hat{r}_q \sum_k P_q(t) \left(\hat{r}_k \rho \hat{r}_k^\dagger + \hat{r}_k^\dagger \rho \hat{r}_k - \hat{r}_k^\dagger \hat{r}_k \rho - \rho \hat{r}_k \hat{r}_k^\dagger \right) \right\} = P_q(t), \quad (\text{A9})$$

where $P_q(t)$ corresponds to an incoherent pumping rate of a single reservoir state. Considering identical reservoir states, we can write equation for the total reservoir occupation as

$$\left. \frac{\partial N_R}{\partial t} \right|_{pump} = \sum_q \left. \frac{\partial n_q^R}{\partial t} \right|_{pump} = \sum_q P_q(t) \equiv P(t), \quad (\text{A10})$$

where we defined the total incoherent pumping rate $P(t)$ as a sum of single state pumps.

Combining the all contributions, for the time dynamics we come to the system of coupled equations (4)-(7).

-
- ¹ O. Kyriienko, A. V. Kavokin, and I. A. Shelykh, Phys. Rev. Lett. **111**, 176401 (2013). and T. C. H. Liew, Phys. Rev. B **90**, 125407 (2014).
- ² O. Kyriienko, E. Ostrovskaya, O. A. Egorov, I. A. Shelykh,